Edward C. Benzel[1]
Department of Neurosurgery,
Neurological Institute,
Cleveland Clinic,
9500 Euclid Avenue, S40,
Cleveland, OH 44195
e-mail: benzele@ccf.org

Isador H. Lieberman
Scoliosis and Spine Tumor Center,
Texas Back Institute,
Texas Health Presbyterian Hospital Plano,
6020 West Parker Road,
Plano, TX 75093
e-mail: ilieberman@texasback.com

E. Raymond Ross
Salford Royal NHS Foundation Trust University
Teaching Hospital,
Stott Lane,
Salford M6 8HD, UK
e-mail: ersross@hotmail.co.uk

Raymond J. Linovitz
CORE Orthopaedic Medical Group,
332 Santa Fe Drive,
Suite 110,
Encinitas, CA 92024
e-mail: doclino@sbcglobal.net

James Kuras
e-mail: jkuras@axiomed.com

Kari Zimmers
e-mail: kzimmers@axiomed.com

AxioMed Spine Corporation,
Garfield Heights, OH 44125

Mechanical Characterization of a Viscoelastic Disc for Lumbar Total Disc Replacement

A viscoelastic artificial disc may more closely replicate normal stiffness characteristics of the healthy human disc compared with first-generation total disc replacement (TDR) devices, which do not utilize viscoelastic materials and are based on a ball and socket design that does not allow loading compliance. Mechanical testing was performed to characterize the durability and range of motion (ROM) of an investigational viscoelastic TDR (VTDR) device for the lumbar spine, the Freedom® Lumbar Disc. ROM data were compared with data reported for the human lumbar disc in the clinical literature. Flexibility and stiffness of the VTDR in compression, rotation, and flexion/extension were within the parameters associated with the normal human lumbar disc. The device constrained motion to physiologic ranges and replicated normal stress/strain dynamics. No mechanical or functional failures occurred within the loads and ROM experienced by the human disc. Fatigue testing of the worst case VTDR device size demonstrated a fatigue life of 50 years of simulated walking and 240 years of simulated significant bends in both flexion/extension and lateral bending coupled with axial rotation, with no functional failures. These results indicate that the VTDR evaluated in this mechanical study is durable and has the ability to replicate the stiffness and mechanics of the natural, healthy human lumbar disc. [DOI: 10.1115/1.4003536]

Keywords: lumbar spine, disc arthroplasty, viscoelastic, disc degeneration, total disc replacement, intervertebral disc, artificial disc

1 Introduction

Restoration of the normal spine function is a goal of lumbar disc degeneration treatment. Although symptomatic disc degeneration can often be medically treated, some patients who have exhausted these measures will seek surgical care. Spinal fusion is the current mainstay of therapy for patients who require surgical intervention for back pain resulting from disc degeneration. However, despite the large number of spinal fusion operations performed annually in the U.S. (nearly 350,000 in 2005) [1], an estimated 25–30% of lumbar fusion patients will not experience any clinical benefits with this procedure [2–5]. In addition, spinal fusion procedures have been associated with complications such as bone graft donor site pain [2,6], pseudoarthrosis [2], and accelerated degeneration of the disc at levels adjacent to the fused vertebrae [7,8].

In recent years, total disc replacement (TDR) has been introduced as another option for the surgical treatment of back pain resulting from disc degeneration. Since 2004, two lumbar TDR devices have been approved in the U.S.: the Charité III (DePuy Spine, Inc., Raynham, MA) and the ProDisc™-L (Synthes Spine, Inc., West Chester, PA). Both utilize a ball and socket design, which represents a modification of hip and knee replacement devices. Newer devices based on this design, specifically the Maverick™ (Medtronic Sofamor Danek, Inc., Memphis, TN), FlexiCore® (Stryker Spine, Allendale, NJ), and Kineflex® (Spinal Motion, Mountain View, CA) artificial discs, are being evaluated in human clinical trials.

TDR may offer advantages over conventional spinal fusion procedures by preserving the function of the spine, which is believed to reduce the risk of adjacent segment degeneration [9–13]. Unlike lumbar fusion, where the goal limits spinal motion, TDR seeks to preserve the segmental range of motion (ROM) [14]. Clinical outcomes for TDR using the approved first-generation devices have been shown to be comparable to [15,16], but not superior to [17,18], outcomes obtained with lumbar fusion.

The natural, healthy human lumbar spinal joint is semiconstrained, with complex three-dimensional movements present in flexion and extension, lateral bending, rotation, and compression, while the viscoelastic human disc [19,20] provides stiffness (passive restraint) and dampening. Ideally, a TDR device should replicate these conditions by

- replicating anatomy (e.g., restoration of disc interspace height and lordotic angle)
- replicating three-dimensional motion in flexion/extension,

[1]Corresponding author.
Manuscript received August 17, 2010; final manuscript received January 13, 2011; published online March 8, 2011. Assoc. Editor: Ted Conway.

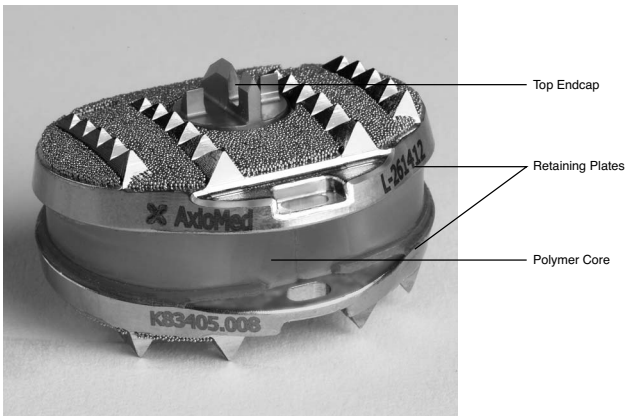

Fig. 1 The FLD VTDR device consisting of titanium alloy end caps and retaining plates with a viscoelastic polymer core

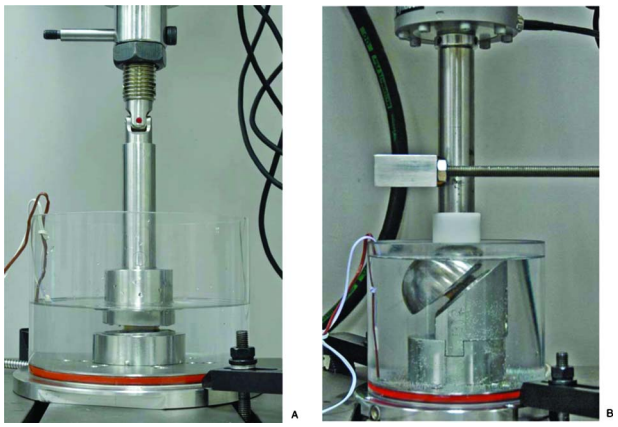

Fig. 2 (*a*) Test configuration for the axial compression and torsion ROM testing using the INSTRON 8874 bi-axial table top servohydraulic dynamic testing system (INSTRON, Canton, MA) in an environmental chamber holding PBS. (*b*) Test configuration for dynamic shear compression tests using the INSTRON 8874 axial table top servohydraulic dynamic testing system (INSTRON, Canton, MA) in PBS.

lateral bending, rotation, and axial compression
- replicating normal spinal mechanics (e.g., stiffness and shock absorption)
- having a low complication rate (e.g., mechanical failure and loosening at the implant/bone interface)
- preventing accelerated degenerative changes at index and adjacent levels
- providing symptom relief
- demonstrating durability and longevity
- providing acceptable revision strategies

One limitation of first-generation TDR devices is that they do not replicate the anatomy, motion, and mechanics of the natural disc and spinal segment. The ball and socket design cannot restore disc angle and does not provide for axial compression. Devices based on this design are only capable of restoring two-dimensional motion, providing load transfer rather than load dampening. In addition, lacking viscoelastic properties, these devices do not constrain the motion of the spinal segment in the same manner as the healthy disc, instead keeping the spine in a state of instability. This characteristic obligates continuous intrinsic reflexive myofascial activity to maintain some measure of normal stability.

Viscoelastic TDR (VTDR) devices, e.g., those designed based on lumbar disc morphology as a one-piece unit with a viscoelastic core bonded to the endplates, may offer advantages compared with first-generation devices by more closely replicating the viscoelastic characteristics of the human disc. Viscoelastic materials exhibit both viscous and elastic characteristics when undergoing deformation, and they exhibit time-dependent strain; i.e., the viscoelastic characteristics of the human disc result in it having increasing stiffness with either increasing loads or increasing loading rate. A TDR with viscoelastic properties would potentially preserve the physiological ROM of the spinal segment and closely mimic the dynamic stiffness and load sharing characteristics of the natural, healthy disc. Several viscoelastic lumbar TDRs are under development, with three currently marketed outside of the U.S.

The aim of the present study was to determine the mechanical characteristics of a new investigational VTDR device under simulated motion and loading conditions and to compare these characteristics to those of the healthy lumbar intervertebral disc.

2 Materials and Methods

2.1 Materials. The Freedom® Lumbar Disc (FLD) (AxioMed Spine Corporation, Garfield Heights, OH) (Fig. 1) is a one-piece investigational lumbar VTDR device. The device's titanium alloy retaining plates are porous coated on both sides. A titanium bead coating on the bone interface side of the retaining plates provides a surface for boney in-growth and long-term fixation, while beads on the polymer interface side provide a surface for mechanical locking with the polymer core. A titanium alloy end cap mechanically locks into each retaining plate through a circular aperture on the plate. The bone interface side of each end cap has a primary fin and two transverse rails that provide short-term fixation with the vertebral endplates. The polymer interface side of the end cap is domed to provide support to the core under high loads. The device's viscoelastic polymer core is composed of thermoplastic silicone polycarbonate urethane (CarboSil™ (The Polymer Technology Group, Berkeley, CA)) bonded mechanically and chemically to the retaining plates.

2.2 Methods. Testing was conducted per the American Society for Testing Materials (ASTM) standard guidelines for the testing of total disc replacement devices [21,22], where applicable. Per the guideline for functional, kinematic, and wear assessment of TDRs [21], functional failure was defined as permanent deformation or wear that renders the intervertebral disc prosthesis assembly ineffective or unable to resist load/motion or any secondary effects that result in a reduction of clinically relevant motions or the motions intended by the device; mechanical failure was defined as failure associated with a defect in the material (e.g., fatigue crack) or failure of the bonding between materials that may or may not produce functional failure.

Testing was conducted on the "worst case" device size (26×36 mm^2, 13 mm, and 12 deg), which has the smallest footprint, smallest polymer volume, and smallest posterior height combination. ROM analyses were also conducted on the largest device size available at the time (28×38 mm^2, 16 mm, and 12 deg) to bracket the stiffness and ROM data for the entire size family. Each specimen was hydrated in phosphate buffered saline (PBS) held at $37 \pm 3\,^{\circ}$C for a minimum of 3 days prior to testing. All testing was conducted in a physiologic ($37 \pm 3\,^{\circ}$C PBS) environment.

For each test, the device was placed into steel fixtures in a servohydraulic load frame and tested in one of the mechanical modes, as described below. An example of the servohydraulic test machinery is shown in Figs. 2(*a*) and 2(*b*).

Mar-Test Inc. (Cincinnati, OH) performed testing of ROM in flexion/extension and wear testing. All other tests were performed by Empirical Testing Corp. (Colorado Springs, CO).

2.3 Range of Motion Tests. The ROM of the VTDR was studied to characterize the stiffness and motion of the device under physiologic loads in compression, rotation, and flexion/extension.

2.4 ROM in Compression and Rotation. Ten devices were tested for ROM in static and dynamic axial compression and static and dynamic torsion using an INSTRON 8874 bi-axial table top servohydraulic dynamic testing system (INSTRON, Norwood, MA).

The axial compression and torsion ROM test steps included quasi-static ramps and short-term fatigue tests at physiologic loads ranging from 400 N to 2000 N in compression and ±6 N m in torsion.

Data analysis included the displacement (ROM) during each test, the static stiffness of each specimen in the range of 400–600 N (axial compression) or ±4 N m (torsion), the dynamic stiffness for one cycle and averaged over the last five recorded cycles, and the hysteresis of the 90th cycle (axial compression) or 190th cycle (torsion).

2.5 ROM in Flexion/Extension. Ten devices were tested in flexion/extension using an MTS 810 servohydraulic closed loop test system (MTS, Eden Prairie, MN).

The flexion/extension ROM test steps included quasi-static ramps and short-term fatigue tests at physiologic loads ranging from 8 N m in flexion to 6 N m in extension.

Data analysis included static stiffness, displacement (ROM), hysteresis at the 400th cycle, and dynamic stiffness from the 380th to 420th cycles. Stiffness was calculated in the total loading range of 8 N m to −6 N m.

2.6 Static Compression Testing. Static compression testing was conducted following ASTM F2346 [22] using an INSTRON 8874 bi-axial table top servohydraulic dynamic testing system to evaluate the stiffness of the device and to determine the compressive strength of the worst case device size. Five devices were tested in displacement control at a rate of 0.2 mm/s until a load cell limit of 20,000 N was reached. Data collection included maximum loads, displacements at maximum load, stiffness within the physiologic loading range, and description of failures.

2.7 Fatigue Testing

2.7.1 Compression. Eight devices were tested in dynamic axial compression per ASTM F2346 [22] to evaluate device durability. The INSTRON 8872 axial table top servohydraulic dynamic testing system (INSTRON, Norwood, MA) was used to apply a cyclic load with a constant frequency of 3 Hz to each specimen. Load values were chosen to develop a well-defined fatigue curve, and testing was terminated when the specimen experienced a functional failure or reached 10×10^6 cycles. Two devices were tested at applied loads of 7000 N and 6000 N to 10×10^6 cycles. Two additional devices were tested in dynamic axial compression with a 2400 N applied load to 50×10^6 cycles at a test frequency of 3 Hz. The failure mode of each device and the corresponding cycle count were recorded.

2.7.2 Compressive Shear. Ten devices were tested in dynamic 45 deg compressive shear to estimate the maximum runout load value at 10×10^6 cycles, as defined by the ASTM F2346 standard [22]. Dynamic shear compression tests were conducted using an INSTRON 8872 axial or 8874 bi-axial table top servohydraulic dynamic testing system. Cyclic loads ranging from 1200 N to 2000 N with a constant frequency of 3 Hz were applied to each specimen to generate a fatigue curve.

Testing was terminated upon either functional failure or completion of 10×10^6 cycles. Dynamic stiffness (force/displacement) was calculated during the first 1000 cycles. The failure location of the specimen and the corresponding cycle count were recorded. A fatigue curve with 95% confidence limits was generated using TABLECURVE 2D (Jandel Scientific, Chicago, IL). In addition, the anterior shear component of the compressive shear load was determined via the following geometric equation: $\cos\theta = a/c$, where θ=compressive shear test angle, a=anterior shear load, and c=compressive shear load.

2.7.3 Wear Testing. Wear testing was conducted using the MTS servohydraulic closed loop test system (MTS, Eden Prairie, MN) to characterize the functional and wear characteristics of the VTDR under coupled motions in flexion/extension/compression and rotation/lateral bending/compression [21].

Six specimens were tested, as well as two controls. Prior to testing, the specimens were weighed and measured for anterior and posterior heights as well as anterior/posterior and lateral lengths and were then hydrated in PBS. The measurements were repeated just prior to testing. The specimens were preconditioned by applying a 1200 N axial load for a minimum of 3 h in PBS. For testing in flexion/extension/compression, the specimens cycled at ±10 N m in flexion/extension under a constant axial compressive load of 1200 N. For testing in rotation/lateral bending/compression, lateral bending was performed in torque control at ±12 N m and axial rotation at ±3 deg in angle control. All tests were performed at a frequency of 2 Hz.

Throughout the testing period, solution samples were collected by MarTest for each test device after each 5×10^6 test machine cycles and sent to BioEngineering Solutions Inc. (Oak Park, IL) for analysis. A total of 20 solution samples were analyzed, and all sample processing was conducted in a class II sterile environment. Each solution was filtered at 0.2 μ, centrifuged to collect the sediment (particles) for further analysis, and ultrasonicated to deflocculate particles.

All particle sizes were given in equivalent spherical diameter based on both number analysis and volume analysis. The number of particles in different particle size ranges was determined. Number analysis provides the percentage of particles in each range by particle number, where volume analysis provides the percentage of particles in each range by mass. Scanning electron microscopy (SEM) with energy-dispersive X-ray analysis (EDXA) was conducted to provide the number based analysis. SEM methods generally only identify the most numerous particles and thus are biased toward smaller particles identified in high magnification images because their average is typically weighted at over 10,000 times that of the low magnification SEM images for distribution calculations. SEM analysis provides for an indirect calculation of total debris per volume and provides a measure of shape (e.g., aspect ratio). Laser diffraction particle analysis (low angle laser light scattering (LALLS)) measures millions to billions of particles and was thus conducted to provide a volume analysis of particle size.

3 Results

3.1 ROM. ROM testing in these mechanical studies demonstrated that the device has stiffness and ROM similar to that of the human lumbar disc (Table 1). There were no mechanical or functional failures of any device size during ROM testing.

3.2 Static Compression. During static testing in axial compression, stiffness increased in a nonlinear fashion with increasing load (Fig. 3).

All devices reached the limit of the test machine load cell with no mechanical or functional failures. The mean displacement at 20,000 N was 3.36 mm.

3.3 Fatigue Testing Studies. Fatigue testing results are summarized in Table 2.

3.3.1 Compression. The worst case device size survived 50×10^6 cycles of axial compression at 2400 N with no mechanical or functional failures. Mechanical and functional failures of the test devices occurred in axial compression at supraphysiologic loads ranging from 6000 N to 17,500 N. The fatigue curve for axial compression testing is shown in Fig. 4. The disc did not functionally fail after 10×10^6 cycles at an axial compressive load of 6000 N. The dynamic stiffness of devices tested to 10×10^6 and 50×10^6 cycles in axial compression remained constant throughout testing (Fig. 5).

Table 1 ROM in the human lumbar disc and mechanical tests of the VTDR device

Parameter	VTDR results[a]	Properties of human lumbar disc
	ROM in compression	
Stiffness	1.55–3.48 kN/mm	0.5–2.5 kN/mm [23–27]
ROM	0.7–1.3 mm under 2000 N load	0.8 mm under 330 N load [28]
	ROM in rotation	
Stiffness	0.72–0.83 N m/deg[b]	2.0–9.6 N m/deg [25,26,29]
ROM	7.6–8.4 deg under 6 N m moment	0–2 deg in healthy volunteers [30]; 1–5.8 deg in cadavers [25,31,32]
	ROM in flexion/extension	
Stiffness	Flexion: 1.4–2.12 N m/deg; extension: 1.4–2.14 N m/deg	Flexion: 0.8–2.5 N m/deg [26]; extension: 2.1 N m/deg [26]
ROM	Flexion: 3.0–5.3 deg at 8 N m moment; extension: 1.9–5.0 deg at 6 N m moment	Flexion: 5.5–13 deg [29,30,33]; extension: 1–5 deg [29,30,33]

[a]For worst case to large sized devices.
[b]For family of device sizes.

3.3.2 Compressive Shear. The same worst case device size survived 10×10^6 cycles at an anterior shear load of 1697 N with no mechanical or functional failures. The fatigue curve for the device tested in 45 deg compressive shear is shown in Fig. 6.

3.3.3 Wear Testing. Wear testing to a total of 30×10^6 device cycles (10×10^6 flexion/extension, 10×10^6 lateral bending, and 10×10^6 rotation) resulted in no functional failures of any worst case sized device. Test specimen analysis data show that the devices lost an average of 0.07 g weight over 30×10^6 device cycles of wear testing. Dimensionally, the devices lost an average of 0.31 mm anterior height and 0.24 mm posterior height over 30×10^6 cycles, while the periphery dimension increased by means of 0.83 mm laterally and 0.64 mm in anterior/posterior.

Particulate analysis revealed an average wear rate (average mass of particulate per million cycles of wear testing) of 1.70 mg per million cycles. For the 20 solution samples tested, the number average particle diameter was 1.90 μm, with a range of 0.80–6.92 μm, and the weight average particle diameter was 48.66 μm, with a range of 23–76 μm.

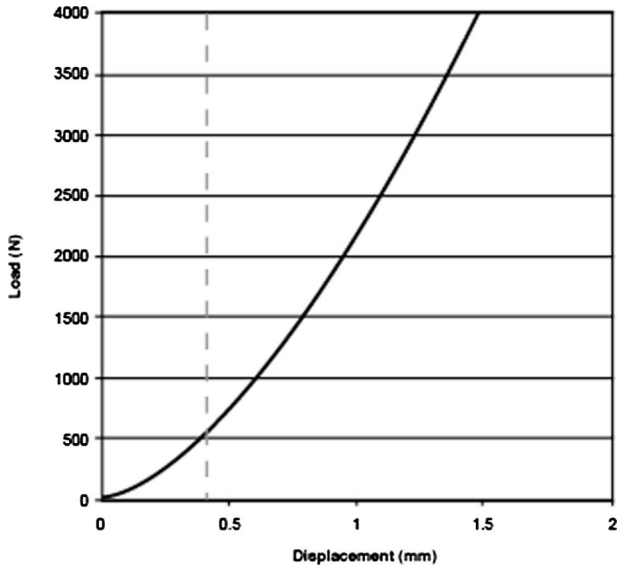

Fig. 3 Results of static testing in axial compression. Data points are plotted and appear as a line. Device stiffness increases with an increasing load. Vertical dashed line at 0.4 mm marks estimated boundary of neutral (high flexibility) (left of line) versus elastic (high stiffness) (right of line) zone.

4 Discussion

Other studies have demonstrated that the ROM of currently approved TDRs is comparable to the ROM of the healthy lumbar intervertebral disc [17,34–37]. However, the present authors found no published studies showing a TDR that mimics the func-

Table 2 Fatigue test results for the VTDR device

Parameter	VTDR results
Compression	• 50×10^6 cycles at 2400 N load (two devices) with no mechanical or functional failures • 10×10^6 cycles at 6000 N and 7000 N (one device each) with no functional failures • Fatigue curve at loads from 6000–17,500 N
45 deg compressive shear	• 10×10^6 cycles at 1697 N anterior shear (1200 N, 45 deg compressive shear) with no mechanical or functional failures • Fatigue curve at loads of 1697–2828 N anterior shear or 1200–2000 N, 45 deg compressive shear
Wear	• 30×10^6 cycles wear testing (five devices) ○ 10M flexion/extension +10 M lateral bending/10M rotation ±10 N m flexion/extension, ±12 N m lateral bending, ±3 deg rotation, 1200 N compression load, with no functional failures

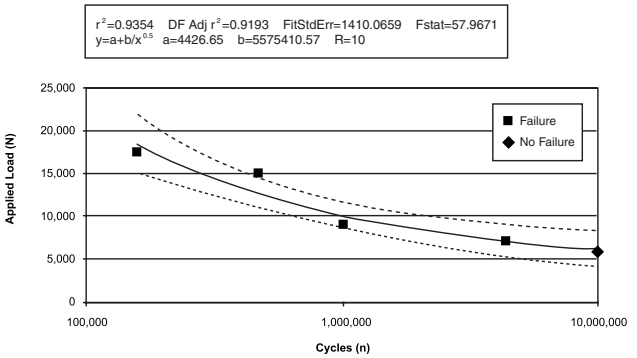

Fig. 4 Axial compression fatigue curve for the VTDR. Data points and 95% confidence interval are shown. Functional failures occurred in axial compression at nonphysiologic loads of 7000–17,500 N.

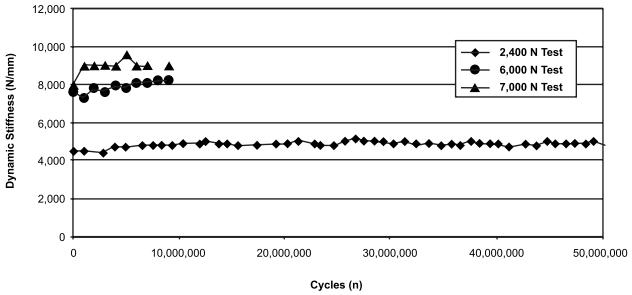

Fig. 5 Dynamic stiffness of the VTDR in axial compression over 10×10^6 and 50×10^6 cycles. Dynamic stiffness of the device remained constant throughout testing, even at the nonphysiologic loads of 6000 N and 7000 N.

tion of the disc in quality or quantity of motion by replicating three-dimensional motion in flexion/extension, lateral bending, rotation, and axial compression, as well as by replicating normal spinal mechanics such as stiffness and shock absorption.

The results of this mechanical study demonstrate that the investigational VTDR device mimics the stiffness and mechanics of the human lumbar disc, with similar quality and quantity of motion, in an in vitro model. Although the VTDR device's stiffness in compression (1.55–3.48 kN/mm) was at the higher end of the range noted in the clinical literature for the healthy human disc (0.5–2.5 kN/mm [23–27]), this may be desirable since this is the primary load-bearing mode of the implant. Stiffness in the higher portion of the reported range may result in the appropriate stability and long-term performance of the implant. In rotation, the VTDR demonstrates stiffness slightly lower (0.72–0.83 N m/deg) than the range reported in the clinical literature for the lumbar disc (2.0–9.6 N m/deg [25,26,28]), resulting in greater ROM for the VTDR compared with the lumbar disc. Although the VTDR does not precisely match the disc stiffness in this loading mode, healthy lumbar discs have a very low ROM in rotation; the VTDR provides this physiologic ROM. The flexibility and stiffness of the VTDR in flexion/extension matched those presented in the clinical literature for the healthy human disc. Overall, the flexibility and stiffness of the VTDR under the various conditions tested in this study are consistent with the clinical literature.

This VTDR was designed to limit motion so that it closely approximates physiologic ranges, which it achieved in these mechanical studies, suggesting its potentially stabilizing effects in in vivo conditions. Both a neutral zone (region of greater flexibility) and an elastic zone (region of greater stiffness) were observed (see Fig. 3), replicating the natural stress/strain dynamics of the human lumbar disc and important for providing physiologic shock absorption during the activities of daily living (ADLs) in vivo. This contrasts with first-generation TDRs in which only a neutral zone exists, without any elastic zone (very low stiffness throughout ROM).

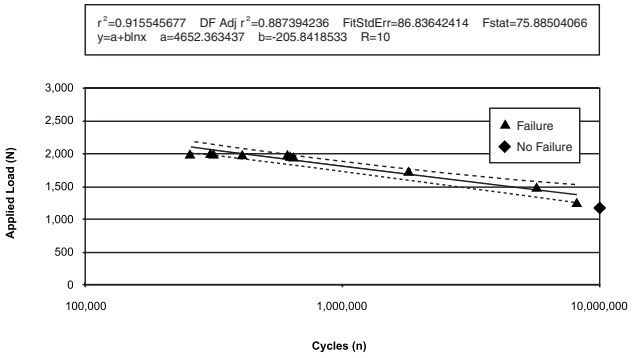

Fig. 6 45 deg compressive shear testing fatigue curve for the VTDR. Data points and 95% confidence interval are shown. The device demonstrated an endurance limit load of 1200 N in 45 deg compressive shear. 45 deg compressive shear loads of 1200–2000 N correspond to loads in anterior shear of 1697–2828 N.

In this study, ROM and fatigue testing demonstrated that no mechanical or functional failures occur with the loads and within the ROM experienced by the human lumbar disc. All mechanical and functional failures were generated at loads and/or ROM much greater than what would be expected in vivo. Anterior shear forces on the lumbar discs are estimated to be between 25 N and 525 N [26,38,39]. The device demonstrated bond durability and an endurance limit load of 1200 N in 45 deg compressive shear, which corresponds to an anterior shear load of 1697 N. Therefore, the device demonstrated an endurance limit of more than five times the maximum amount of anterior shear that the device would be expected to experience during ADLs in vivo.

The VDTR survived wear testing at 30×10^6 cycles, the equivalent of 240 years of simulated significant bends per the estimate of Hedman et al. [40] of 125,000 significant bends per year in flexion/extension for the typical human lumbar spine, which is widely used to determine simulated life from wear testing. At axial compressive loads in the range of normal ADL loads, each compression fatigue test cycle (used to predict long-term, in vivo performance) simulates a walking step. It is generally believed that the average person takes 1×10^6 steps/year [41,42]; therefore, a 10×10^6 cycle compression fatigue test is used to predict 10 years of simulated in vivo loading. The ADL axial compression load in the lumbar spine is estimated to be 1200 N based on the range of loads during daily activities found by Nachemson [38]. For this study, this estimated ADL was doubled (2400 N) to provide an inherent safety factor for the test. The VDTR devices tested survived 50×10^6 cycles at a 2400 N load, the equivalent of 50 years of simulated walking. Thus, fatigue testing of the worst case device size demonstrated that the device has the durability sufficient to perform in vivo for more than 50 years, with a fatigue life of 50 years of simulated walking, and 240 years of simulated significant bends in both flexion/extension and lateral bending coupled with axial rotation, with no functional failures.

Although the use of different test methodologies prohibits a direct comparison, the wear rate (mass loss/million cycles) of the VTDR (1.70 mg at 30×10^6 cycles, tested using ASTM methods) falls within the range between the wear rates of the Charité III (0.11 mg at 20×10^6 device cycles, tested per ASTM methods [43]) and the ProDisc™-L (5.73 mg at 30×10^6 device cycles, tested per International Organization for Standardization (ISO) methods [44]).

The particle size of the wear debris generated by the VTDR device (1.90 μm number average particle diameter) is larger than the median diameter reported for the Charité (0.2 μg number median particle diameter [43]) and the average diameter reported for the ProDisc (0.44 μm number average particle diameter [44]). A smaller particle size is thought to be associated with a higher rate of pro-inflammatory response compared with larger particles [45]; therefore, the larger particle size of the investigational VTDR device may potentially result in less bioreactivity in vivo compared with existing devices. Particle size and wear generation depend on many factors, including implant design and material composition, test loads, and fluid environments [46]. There are several differences between wear testing of the lumbar VTDR in the present study and that reported for the commercially available TDRs. The available TDRs both have articulating wear surfaces, whereas the VTDR does not, and are comprised of metal and (nonelastomeric) plastic, whereas the VTDR is metal and elastomeric. The testing environment for the commercially available discs was serum, which acts as a lubricant, while the saline test environment used for the VTDR offers no lubrication. All of these

differences may contribute to the difference in wear debris particle size between the VTDR device and the commercially available devices.

Facet pain, facet arthritis, and facet degeneration [35,47–50] have been noted with the first-generation TDR devices and are believed to occur due to the unconstrained motion of the approved ball and socket articulated devices [51], which are designed with low-friction, sliding surfaces comprised of two metal endplates and a polyethylene core [52]. The Charité III device has two articulating surfaces (between the core and both endplates), which allow rotation and limited translation [52,53], while the ProDisc II has only one articulating surface (between the core and the upper plate), which allows rotation but no translation [52]. In contrast, the investigational VTDR device has no articulating surfaces, and the bonding of the core to the endplates provides physiologic motion, including passive constraint. In addition, unlike the polyethylene core of currently approved devices, the polymer core provides compression. These design features allow for three-dimensional motion, provide passive restraint of motion within and limited to the physiologic range, and provide shock absorption that is not available with ball and socket style devices. However, any effect of motion constraint on clinical outcomes for patients receiving viscoelastic implants is hypothetical at this time and will require demonstration in human trials.

This study attempted to compare the properties of a next-generation TDR device, as determined by in vitro mechanical testing, to the properties of the healthy lumbar intervertebral disc presented in in vivo and in vitro studies. This comparison is hindered by small numbers (5–10) of VTDR device samples evaluated in each test, by numerous differences in test methodology among the studies in the clinical literature, and by virtue of these tests being conducted in a mechanical model, rather than a biomechanical (e.g., animal or cadaver) model or clinical study. Further study is needed to determine if in vivo results for the tested device correlate with in vitro results and to determine if statistical differences exist.

5 Conclusions

The one-piece VTDR evaluated in this study, designed based on lumbar disc morphology to exhibit the stiffness characteristics of the natural lumbar disc, represents a next-generation disc for lumbar TDR. These tests demonstrate that the device met its design criteria. The device's mechanical properties replicate the ROM, flexibility, and stiffness (passive constraint) of the healthy human lumbar disc, with durability sufficient to perform in vivo for more than 50 years. Clinical investigation of this VTDR device is warranted.

Acknowledgment

Editorial and administrative support for this manuscript was provided by Danielle M. Briscoe, MPH, Corinth Group Communications, Inc. (New York, NY) and paid for by the study sponsor (AxioMed Spine Corp., Garfield Heights, OH). Administrative support was also provided by Christine M. Moore, Department of Neurosurgery, Cleveland Clinic.

References

[1] Merrill, C., and Elixhauser, A., 2007, "Hospital Stays Involving Musculoskeletal Procedures, 1997–2005," HCUP Statistical Brief No. 34, Agency for Healthcare Research and Quality, Rockville, MD, available at http://www.hcup-us.ahrq.gov/reports/statbriefs/sb34.pdf, accessed Aug. 9, 2010.

[2] Turner, J. A., Ersek, M., Herron, L., Haselkorn, J., Kent, D., Ciol, M. A., and Deyo, R., 1992, "Patient Outcomes After Lumbar Spinal Fusions," JAMA, J. Am. Med. Assoc., **268**(7), pp. 907–911.

[3] Boos, N., and Webb, J. K., 1997, "Pedicle Screw Fixation in Spinal Disorders: A European View," Eur. Spine J., **6**(1), pp. 2–18.

[4] Bono, C. M., and Lee, C. K., 2004, "Critical Analysis of Trends in Fusion for Degenerative Disc Disease Over the Past 20 Years: Influence of Technique on Fusion Rate and Clinical Outcome," Spine, **29**(4), pp. 455–463.

[5] Christensen, F. B., 2004, "Lumbar Spinal Fusion. Outcome in Relation to Surgical Methods, Choice of Implant and Postoperative Rehabilitation," Acta Orthop. Scand. Suppl., **75**(313), pp. 2–43.

[6] Spine Interbody Research Group, Sasso, R. C., LeHuec, J. C., and Shaffrey, C., 2005, "Iliac Crest Bone Graft Donor Site Pain After Anterior Lumbar Interbody Fusion: A Prospective Patient Satisfaction Outcome Assessment," J. Spinal Disord. Tech., **18**, pp. S77–S81.

[7] Park, P., Garton, H. J., Gala, V. C., Hoff, J. T., and McGillicuddy, J. E., 2004, "Adjacent Segment Disease After Lumbar or Lumbosacral Fusion: Review of the Literature," Spine, **29**(17), pp. 1938–1944.

[8] Harrop, J. S., Youssef, J. A., Maltenfort, M., Vorwald, P., Jabbour, P., Bono, C. M., Goldfarb, N., Vaccaro, A. R., and Hilibrand, A. S., 2008, "Lumbar Adjacent Segment Degeneration and Disease After Arthrodesis and Total Disc Arthroplasty," Spine, **33**(15), pp. 1701–1707.

[9] Rahm, M. D., and Hall, B. B., 1996, "Adjacent-Segment Degeneration After Lumbar Fusion With Instrumentation: A Retrospective Study," J. Spinal Disord., **9**(5), pp. 392–400.

[10] Huang, R. C., Girardi, F. P., Cammisa, F. P., Jr., Lim, M. R., Tropiano, P., and Murnay, T., 2005, "Correlation Between Range of Motion and Outcome After Lumbar Total Disc Replacement: 8.6-Year Follow-Up," Spine, **30**, pp. 1407–1411.

[11] Chung, S. S., Lee, C. S., and Kang, C. S., 2006, "Lumbar Total Disc Replacement Using ProDisc II: A Prospective Study With a 2-Year Minimum Follow-Up," J. Spinal Disord. Tech., **19**(6), pp. 411–415.

[12] Huang, R. C., Tropiano, P., Marnay, T., Girardi, F. P., Lim, M. R., and Cammisa, F. P., Jr., 2006, "Range of Motion and Adjacent Level Degeneration After Lumbar Total Disc Replacement," Spine J., **6**(3), pp. 242–247.

[13] Putzier, M., Funk, J. F., Schneider, S. V., Gross, C., Tohtz, S. W., Khodadadyan-Klostermann, C., Perka, C., and Kandziora, F., 2006, "Charite Total Disc Replacement—Clinical and Radiographical Results After an Average Follow-Up of 17 Years," Eur. Spine J., **15**(2), pp. 183–195.

[14] Huang, R. C., Girardi, F. P., Cammisa, F. P., Jr., and Wright, T. M., 2003, "The Implications of Constraint in Lumbar Total Disc Replacement," J. Spinal Disord. Tech., **16**(4), pp. 412–417.

[15] Blumenthal, S., McAfee, P. C., Guyer, R. D., Hochschuler, S. H., Geisler, F. H., Holt, R. T., Garcia, R., Jr., Regan, J. J., and Ohnmeiss, D. D., 2005, "A Prospective, Randomized, Multicenter Food and Drug Administration Investigational Device Exemptions Study of Lumbar Total Disc Replacement With the CHARITE Artificial Disc Versus Lumbar Fusion: Part I: Evaluation of Clinical Outcomes," Spine, **30**(14), pp. 1565–1575.

[16] Lemaire, J.-P., Carrier, H., Ali, E.-H. S., Skalli, W., and Lavaste, F., 2005, "Clinical and Radiological Outcomes With the Charité™ Artificial Disc: A 10-Year Minimum Follow-Up," J. Spinal Disord. Tech., **18**(4), pp. 353–359.

[17] Freeman, B. J. C., and Davenport, J., 2006, "Total Disc Replacement in the Lumbar Spine: A Systematic Review of the Literature," Eur. Spine J., **15**, pp. 439–447.

[18] Krishnaney, A. A., Park, J., and Benzel, E. C., 2007, "Surgical Management of Neck and Low Back Pain," Neurol. Clin., **25**(2), pp. 507–522.

[19] Iatridis, J. C., Weidenbaum, M., Setton, L. A., and Mow, V. C., 1996, "Is the Nucleus Pulposus a Solid or a Fluid? Mechanical Behaviors of the Nucleus Pulposus of the Human Intervertebral Disc," Spine, **21**(10), pp. 1174–1184.

[20] Iatridis, J. C., Setton, L. A., Weidenbaum, M., and Mow, V. C., 1997, "The Viscoelastic Behavior of the Non-Degenerate Human Lumbar Nucleus Pulposus in Shear," J. Biomech., **30**(10), pp. 1005–1013.

[21] ASTM Standard F2423, 2005, "Standard Guide for Functional, Kinematic, and Wear Assessment of Total Disc Prostheses," ASTM International, West Conshohocken, PA.

[22] ASTM Standard F2346, 2005, "Standard Test Methods for Static and Dynamic Characterization of Spinal Artificial Discs," ASTM International, West Conshohocken, PA.

[23] Berkson, M. H., Nachemson, A., and Schultz, A. B., 1979, "Mechanical Properties of Human Lumbar Spine Motion Segments—Part II: Responses in Compression and Shear; Influence of Gross Morphology," ASME J. Biomech. Eng., **101**, pp. 53–75.

[24] Tencer, A. F., Ahmed, A. M., and Burke, D. L., 1982, "Some Static Mechanical Properties of the Lumbar Intervertebral Joint, Intact and Injured," ASME J. Biomech. Eng., **104**(3), pp. 193–201.

[25] White, A. A., III, and Panjabi, M. M., 1990, *Clinical Biomechanics of the Spine*, 2nd ed., Lippincott Williams & Wilkins, Philadelphia, PA, pp. 9 and 107.

[26] Eijkelkamp, M. F., van Donkelaar, C. C., van Horn, J. R., Huyghe, J. M., and Verkerke, G. J., 2001, "Requirements for an Artificial Intervertebral Disc," Int. J. Artif. Organs, **24**(5), pp. 311–321.

[27] Li, S., Patwardhan, A. G., Amirouche, F. M., Havey, R., and Meade, K. P., 1995, "Limitations of the Standard Linear Solid Model of Intervertebral Discs Subject to Prolonged Loading and Low-Frequency Vibration in Axial Compression," J. Biomech., **28**(7), pp. 779–790.

[28] Kimura, S., Steinbach, G. C., Watenpaugh, D. E., and Hargens, A. R., 2001, "Lumbar Spine Disc Height and Curvature Responses to an Axial Load Generated by a Compression Device Compatible With Magnetic Resonance Imaging," Spine, **26**(23), pp. 2596–2600.

[29] Schultz, A. B., Warwick, D. N., Berkson, M. H., and Nachemson, A. L., 1979, "Mechanical Properties of Human Lumbar Spine Motion Segments—Part I: Responses in Flexion, Extension, Lateral Bending, and Torsion," ASME J. Biomech. Eng., **101**, pp. 46–52.

[30] Pearcy, M., Portek, I., and Shepherd, J., 1984, "Three-Dimensional X-Ray Analysis of Normal Movement in the Lumbar Spine," Spine, **9**(3), pp. 294–297.

[31] Panjabi, M., Henderson, G., Abjornson, C., and Yue, J., 2007, "Multidirec-

tional Testing of One- and Two-Level ProDisc-L Versus Simulated Fusions," Spine, **32**(12), pp. 1311–1319.
[32] Panjabi, M., Malcolmson, G., Teng, E., Tominaga, Y., Henderson, G., and Serhan, H., 2007, "Hybrid Testing of Lumbar CHARITÉ Discs Versus Fusions," Spine, **32**(9), pp. 959–966.
[33] Phillips, F. M., Cunningham, B., Carandang, G., Ghanayem, A. J., Voronov, L., Havey, R. M., and Patwardhan, A. G., 2004, "Effect of Supplemental Translaminar Facet Screw Fixation on the Stability of Stand-Alone Anterior Lumbar Interbody Fusion Cages Under Physiologic Compressive Preloads," Spine, **29**(16), pp. 1731–1736.
[34] McAfee, P. C., Cunningham, B., Holsapple, G., Adams, K., Blumenthal, S., Guyer, R. D., Dmietriev, A., Maxwell, J. H., Regan, J. J., and Isaza, J., 2005, "A Prospective, Randomized, Multicenter Food and Drug Administration Investigational Device Exemption Study of Lumbar Total Disc Replacement With the CHARITÉ Artificial Disc Versus Lumbar Fusion: Part II: Evaluation of Radiographic Outcomes and Correlation of Surgical Technique Accuracy With Clinical Outcomes," Spine, **30**(14), pp. 1576–1583.
[35] David, T., 2007, "Long-Term Results of One-Level Lumbar Arthroplasty: Minimum 10-Year Follow-Up of the CHARITÉ Artificial Disc in 106 Patients," Spine, **32**(6), pp. 661–666.
[36] Zigler, J., Delamarter, R., Spivak, J. M., Linovitz, R. J., Danielson, G. O., III, Haider, T. T., Cammisa, F., Zuchermann, J., Balderston, R., Kitchel, S., Foley, K., Watkins, R., Bradford, D., Yue, J., Yuan, H., Herkowitz, H., Geiger, D., Bendo, J., Peppers, T., Sachs, B., Girardi, F., Kropf, M., and Goldstein, J., 2007, "Results of the Prospective, Randomized, Multicenter Food and Drug Administration Investigational Device Exemption Study of the ProDisc-L Total Disc Replacement Versus Circumferential Fusion for the Treatment of 1-Level Degenerative Disc Disease," Spine, **32**(11), pp. 1155–1162.
[37] Guyer, R. D., McAfee, P. C., Banco, R. J., Bitan, F. D., Cappuccino, A., Geisler, F. H., Hochschuler, S. H., Holt, R. T., Jenis, L. G., Majd, M. E., Regan, J. J., Tromansauser, S. G., Wong, D. C., and Blumenthal, S. L., 2009, "Prospective, Randomized, Multicenter Food and Drug Administration Investigational Device Exemption Study of Lumbar Total Disc Replacement With the CHARITE Artificial Disc Versus Lumbar Fusion: Five-Year Follow-Up," Spine J., **9**(5), pp. 374–386.
[38] Nachemson, A. L., 1981, "Disc Pressure Measurements," Spine, **6**(1), pp. 93–97.
[39] Han, J. S., Goel, V. K., Ahn, J. Y., Winterbottom, J., McGowan, D., Weinstein, J., and Cook, T., 1995, "Loads in the Spinal Structures During Lifting: Development of a Three-Dimensional Comprehensive Biomechanical Model," Eur. Spine J., **4**(3), pp. 153–168.
[40] Hedman, T. P., Kostuik, J. P., Fernie, G. R., and Heller, W. G., 1991, "Design of an Intervertebral Disc Prosthesis," Spine, **16**(6), pp. S256–S260.
[41] Schmalzried, T. P., Szuszczewicz, E. S., Northfield, M. R., Akizuki, K. H., Frankel, R. E., Belcher, G., and Amstutz, H. C., 1998, "Quantitative Assessment of Walking Activity After Total Hip or Knee Replacement," J. Bone Jt. Surg., Am. Vol., **80**(1), pp. 54–59.
[42] Morlock, M., Schneider, E., Bluhm, A., Vollmer, M., Bergmann, G., Muller, V., and Honl, M., 2001, "Duration and Frequency of Every Day Activities in Total Hip Patients," J. Biomech., **34**(7), pp. 873–881.
[43] U.S. Food and Drug Administration, 2004, "Summary of Safety and Effectiveness Data: CHARITÉ Artifical Disc," available at http://www.accessdata.fda.gov/cdrh_docs/pdf4/P040006b.pdf, accessed May 25, 2010.
[44] U.S. Food and Drug Administration, 2006, "Summary of Safety and Effectiveness Data: PRODISC®-L Total Disc Replacement," available at http://www.accessdata.fda.gov/cdrh_docs/pdf5/P050010b.pdf, accessed May 25, 2010.
[45] Jacobs, J. J., Hallab, N. J., Urban, R. M., and Wimmer, M. A., 2006, "Wear Particles," J. Bone Jt. Surg., Am. Vol., **88**, pp. 99–102.
[46] Harper, M. L., Dooris, A., and Paré, P. E., 2009, "The Fundamentals of Biotribology and Its Application to Spine Arthroplasty," SAS J., **3**(4), pp. 125–132.
[47] van Ooij, A., Oner, F. C., and Verbout, A. J., 2003, "Complications of Artificial Disc Replacement: A Report of 27 Patients With the SB Charité Disc," J. Spinal Disord. Tech., **16**(4), pp. 369–383.
[48] Phillips, F., Diaz, R., and Pimenta, L., 2005, "The Fate of the Facet Joints After Lumbar Total Disc Replacement: A Clinical and MRI Study," Spine J., **5**(4), p. S75.
[49] Lemaire, J. P., Skalli, W., Lavaste, F., Templier, A., Mendes, F., Diop, A., Sauty, V., and Laloux, E., 1997, "Intervertebral Disc Prosthesis. Results and Prospects for the Year 2000," Clin. Orthop. Relat. Res., **337**, pp. 64–76.
[50] Shim, C. S., Lee, S. H., Shin, H. D., Kang, H. S., Choi, W. C., Jung, B., Choi, G., Ahn, Y., Lee, S., and Lee, H. Y., 2007, "Charité Versus ProDisc: A Comparative Study of a Minimum 3-Year Follow-Up," Spine, **32**(9), pp. 1012–1018.
[51] Park, C. K., Ryu, K. S., and Jee, W. H., 2008, "Degenerative Changes of Discs and Facet Joints in Lumbar Total Disc Replacement Using ProDisc II: Minimum Two-Year Follow-Up," Spine, **33**(16), pp. 1755–1761.
[52] de Kleuver, M., Oner, F. C., and Jacobs, W. C., 2003, "Total Disc Replacement for Chronic Low Back Pain: Background and a Systematic Review of the Literature," Eur. Spine J., **12**(2), pp. 108–116.
[53] Link, H. D., 2002, "History, Design and Biomechanics of the LINK SB Charité Artificial Disc," Eur. Spine J., **11**, pp. S98–S105.